

# Encapsulation of an Anionic Surfactant into Hollow Spherical Nanosized Capsules: Size Control, Slow Release, and Potential Use for Enhanced Oil Recovery Applications and Environmental Remediation

Ahmed Wasel Alsmail, Mohammed Amen Hammami, Apostolos Enotiadis, Mazen Yousef Kanj, and Emmanuel P. Giannelis\*

Cite This: <https://dx.doi.org/10.1021/acsomega.0c06094>

Read Online

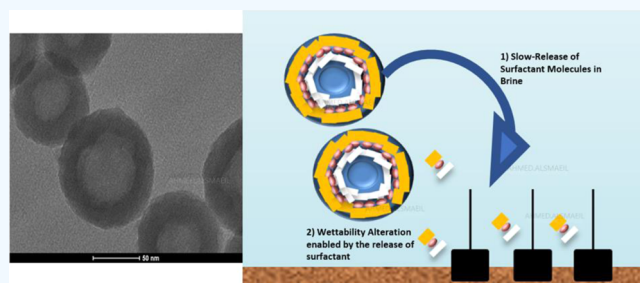
ACCESS |

Metrics & More

Article Recommendations

Supporting Information

**ABSTRACT:** A new platform that allows encapsulation of anionic surfactants into nanosized capsules and subsequent release upon deployment is described. The system is based on DOWFAX surfactant molecules incorporated into sub-100 nm hollow silica nanoparticles composed of a mesoporous shell. The particles released 40 wt % of the encapsulated surfactant at 70 °C compared to 24 wt % at 25 °C after 21 and 18 days, respectively. The use of the particles for subsurface applications is assessed by studying the effectiveness of the particles to alter the wettability of hydrophobic surfaces and reduction of the interfacial tension. The release of the surfactant molecules in the suspension reduces the contact angle of a substrate from 105 to 25° over 55 min. A sustained release profile is demonstrated by a continuous reduction of the interfacial tension of an oil suspension, where the interfacial tension is reduced from 62 to 2 mN m<sup>-1</sup> over a period of 3 days.



## INTRODUCTION

Surfactant injection and delivery has been extensively utilized as one of the most efficient approaches for chemical enhanced oil recovery (cEOR) and for environmental applications including oil spill remediation as well as enhancing solubilization of soil contaminants. The surfactants can reduce interfacial tension (IFT) and alter the wettability of hydrophobic surfaces.<sup>1–7</sup> A key limitation of this approach is premature adsorption and consumption of the surfactant molecules, which requires deployment of a substantially larger amount from that needed.<sup>8–11</sup> For example, sodium dodecyl sulfate (SDS) molecules adsorb preferentially to carbonate surfaces present in oil reservoirs via electrostatic interactions between the divalent Ca<sup>2+</sup> ions and the negatively charged surfactant.<sup>11</sup>

To that end, several groups started exploring the use of nanoparticles to deliver surfactants as a means to reduce surfactant losses. For example, Zhong et al. have reported LUDOX nanoparticles with a nonionic surfactant, which resulted in reducing the adsorption to rock powders.<sup>12</sup> Others reported using SiO<sub>2</sub> nanoparticles to reduce SDS adsorption.<sup>13</sup> They found that the concentration of the nanoparticles affects the amount of surfactant adsorption.<sup>13</sup> However, these approaches do not offer a sustainable or controlled release mechanism of surfactants to targeted locations. Moreover, the physically adsorbed surfactant by the carrying nanoparticles

may be susceptible to losses and instability as the particles diffuse in the porous medium. Other researchers explored the addition of sacrificial chemicals to lower the adsorption of surfactants to the reservoir minerals but these chemicals could be costly for field operations.<sup>7</sup> To overcome this limitation, the use of the slow release of surfactant molecules (similar to slow release of drugs carried by nanoparticles for therapy) has emerged as one of the promising solutions to circumvent surfactant losses and instability for subsurface applications.

One such approach is encapsulation of surfactants into a compatible host. For example, one of the earliest proof-of-concept demonstrations on reducing surfactant adsorption by encapsulation was made by Kittirisawai and Romero-Zerón. They reported the successful incorporation of SDS into  $\beta$ -cyclodextrin. Their system resulted in reducing SDS adsorption by as much as 74%.<sup>14</sup> More recently, other researchers have reported the encapsulation of surfactants in micron-sized double emulsions.<sup>15</sup> Beeswax shell, which allowed encapsulation of nonionic surfactants,<sup>16</sup> and type II resins isolated from

Received: December 16, 2020

Accepted: February 10, 2021

vacuum residue were used as a shell for Span 20 and Petro 50 surfactants.<sup>17</sup> However, previous studies did not provide kinetic studies of surfactant release or demonstrate a controlled mechanism for surfactant diffusion from the host materials. Moreover, some of the reported materials may not be suitable for high-temperature environments.<sup>17</sup> More importantly, previous studies were not conducted at conditions representative of the subsurface environment, especially in terms of salinity.

Mesoporous materials represent a potential host platform that could be utilized to encapsulate surfactants. Since their discovery, mesoporous materials have attracted widespread interest in many applications such as drug delivery and biosensing,<sup>18–20</sup> water treatment,<sup>21,22</sup> catalysis,<sup>23,24</sup> and protective coatings.<sup>25</sup> Among mesoporous materials, silica-based mesoporous materials are promising due to their stability and availability. During the synthesis, the surfactant is used as a template and co-structure directing agent. However, the surfactant is then typically extracted thermally or chemically and the surfactant-free particles offer well-controlled mesoporous systems used as catalyst supports or sorbents.<sup>10,18–26</sup>

Despite their widespread uses, there are only limited reports on utilizing mesoporous materials for hydrocarbon recovery or remediation applications. de Freitas et al. proposed using a class of mesoporous materials (SBA-15) to control the delivery of surfactants for subsurface applications. They utilized a nonionic surfactant that binds to the surface of the particles and slowly desorbs into water–oil mixtures to lower the IFT of the oil–water interface.<sup>27</sup> However, in their study, they extracted the Pluronic 123 surfactant used as a template in the synthesis and relied on physically adsorbed fatty diethanolamides, which due to the weak interaction between the surfactant and the silica surface, can dissociate easily and suffer from the same loss issues as the neat surfactant injected directly into the reservoir.

Recently, we demonstrated in a preliminary study that mesoporous nanoparticles can indeed offer an effective platform for controlling the release of cationic surfactants present in the mesoporous host. In a proof-of-concept experiment, mesoporous silica (MCM-41) has been used as the host to deliver the encapsulated cationic surfactant by ion exchange with the ions available in high-salinity water (HSW).<sup>28</sup> One limitation of this approach, however, is that the typical synthesis of MCM-41 is based on cationic surfactants as templates, which does not subject itself to encapsulation of anionic molecules. Most of the work for the synthesis of mesoporous silica hosts has been devoted to using cationic and nonionic surfactants as templates.<sup>29–34</sup> Here, we extend our previous work and focus on encapsulating anionic surfactant molecules into the pores of nanosized mesoporous silica hollow particles. Incorporation of anionic surfactants as templates for the mesoporous host requires careful selection of the silica precursor and modification of the reaction conditions. To that end, (3-aminopropyl) triethoxysilane (APTES) is added along with tetraethyl orthosilicate (TEOS) as silica precursors. The presence of a positively charged group on APTES provides the anchor group for interactions with the negatively charged surfactant molecules.<sup>26</sup>

DOWFAX represents a family of commercially available anionic surfactants (Figure S1), which have been studied extensively for subsurface oil and environmental remediation applications including solubilization of soil contaminants.<sup>35,36</sup> It is believed that due to the presence of the sulfonate groups,

it is stable in brines containing divalent calcium ions up to 0.1 M.<sup>37</sup> It has received attention for cEOR application starting in the 1970s as it proved effective in enhancing oil recovery and demonstrated stability in the presence of both monovalent and divalent ions. Furthermore, it had shown effectiveness in improving the oil recovery by 25% from Berea sandstone rock.<sup>38</sup> However, no previous attempts were made to encapsulate the surfactant for slow release.

In this paper, we demonstrate a platform for the slow release of one of the DOWFAX surfactants, DOWFAX 2A1, an anionic surfactant based on different-sized hollow silica nanocapsules. We study how the size and morphology of the nanocapsules affect the release of the surfactant. The release is triggered by a reverse ion exchange process with ions present in the injection and formation water. The release is also studied at high-temperature conditions that are normally encountered in the subsurface environment. To demonstrate its applicability for subsurface applications, we further investigate the ability of the nanocapsules to alter the surface wettability and in reducing the IFT with the encapsulated sulfonate surfactant.

## EXPERIMENTAL SECTION

**Materials.** DOWFAX 2A1 was purchased from Dow Chemicals Co. The average molecular weight is 576 with a 45% active ingredient and a density of  $\sim 1.15$  g mL<sup>-1</sup>. The DOWFAX 2A1 was used as a templating agent to synthesize the nanocapsules. TEOS and APTES were purchased from Sigma-Aldrich and used without any purification. Sodium chloride (NaCl), calcium chloride dihydrate (CaCl<sub>2</sub>·2H<sub>2</sub>O), magnesium chloride hexahydrate (MgCl<sub>2</sub>·6H<sub>2</sub>O), sodium sulfate (Na<sub>2</sub>SO<sub>4</sub>), and sodium bicarbonate (NaHCO<sub>3</sub>) were all purchased from Sigma-Aldrich. Dodecane and silicone oil were used for contact angle and IFT measurements. The respective densities at room temperature are 0.75 and 0.99 g mL<sup>-1</sup>.

We utilized a multi-salt brine solution similar to the HSW composition proposed by Abdel-Fattah et al.<sup>39</sup> The preparation was carried out in a 1 L volumetric flask. The composition of the brine is shown in Table 1. The salts were dissolved in 1 L of deionized (DI) water, mixed, and stirred at 40 °C.

**Table 1. Amounts of Salt Used to Prepare the HSW Brine (Amounts in 1 L of DI Water)<sup>a</sup>**

compound	NaCl	CaCl <sub>2</sub> ·2H <sub>2</sub> O	MgCl <sub>2</sub> ·6H <sub>2</sub> O	Na <sub>2</sub> SO <sub>4</sub>	NaHCO <sub>3</sub>
mass (g)	41.04	2.384	17.645	6.343	0.165

<sup>a</sup>Published with permission from Alsmaeil et al.<sup>28</sup> through Copyright Clearance Center, Inc.

**Synthesis of Encapsulated DOWFAX 2A1.** The modified procedure described by Han et al.<sup>40</sup> was employed. DOWFAX 2A1 was dissolved in a mixture of 100 mL of DI water and 10 mL of ethanol at room temperature. The temperature was later increased to 80 °C, and 2.4 mL of TEOS and 0.3 mL of APTES were added dropwise to the mixture. Synthesis parameters such as stirring time, temperature, and molar ratios of DOWFAX 2A1, APTES, and TEOS that affect mean particle size and the amount of the surfactant encapsulated are shown in Table 2. The critical micelle concentration (cmc) of DOWFAX 2A1 in 0.1 M NaCl as reported by the manufacturer is 0.12 mM. During the

Table 2. Synthesis Conditions and Stoichiometries Used for the DOWFAX 2A1 Containing Nanocapsules

recipe #	D_1	D_2	D_3	D_4
molar ratio (H <sub>2</sub> O/ETOH/DOWFAX 2A1/APTES/TEOS)	833/25/1/0.7/2.5	833/25/1/0.7/2.5	926/29/1/0.3/1.3	1159/35.5/1/0.4/0.9
stirring speed (rpm)	0	100	300	400
temperature (°C)	80	80	70	70 (2 h), 25 (22 h)
reaction time (days)	1	1	2	1
size (nm)	260 ± 26	257 ± 34	129 ± 32	52 ± 11
shape	irregular	irregular	spherical	spherical
organic content (%)	29	29	35	42

synthesis, the concentration of DOWFAX 2A1 was kept above the reported cmc.

**Characterization.** Transmission electron microscopy (TEM) images were obtained using a Mira Tescan and Tecnai T12. The powder was dispersed in DI water and dropped into copper grids prior to the measurements. The images were analyzed using ImageJ software to obtain the average particle size. Thermogravimetric analysis (TGA) was performed to quantify the organic content present using Q500 TA Instruments' thermal analyzer with a heating rate of 10 °C min<sup>-1</sup> from 25 to 900 °C under a nitrogen flow (10 mL min<sup>-1</sup>). The instrument has an isothermal accuracy of ±1 °C. The sample was crushed evenly and about 10 mg of the powder was placed on the platinum pan and loaded into the TGA. Fourier-transform infrared (FTIR) spectra were obtained on the Bruker Vertex V80V Vacuum FTIR system with a spectral range of 500–6000 cm<sup>-1</sup> and resolution of 0.02 cm<sup>-1</sup>. The measurements were conducted under vacuum. The size of the pores after extracting the surfactant from the nanocapsules was determined by the Barrett–Joyner–Halenda (BJH) method using nitrogen adsorption on a Micrometrics model ASAP 2460. UV–vis spectra used to quantify the surfactant release were acquired by the plate reader model M2 instrument manufactured by Molecular Devices. Contact angle measurements were performed using a contact angle tester by Biolin Scientific model Theta Lite that has a digital camera that operates with a capability of 2068 frames per second (fps). The instrument can measure the contact angle from 0 to 180° with an accuracy of ±0.1°. The experiments were repeated on different locations of the glass surface. The IFT measurements were performed using a spinning drop tensiometer (SDT) by Kruss. The instrument can measure the IFT from 10<sup>-6</sup> to 2000 mN m<sup>-1</sup> with a resolution of 10<sup>-6</sup> mN m<sup>-1</sup> and a temperature range from ambient to 120°.

**Release Experiments.** The surfactant release was measured by suspending 10 mg of the nanocapsules in 20 mL of HSW and measuring the concentration of the surfactant released by UV–vis spectroscopy. Detailed information is provided in the Supporting Information.

**Wettability Alteration Experiments.** Wettability alteration experiments were performed to evaluate the effectiveness of the system in transforming an oil-wet to a preferred water-wet surface.<sup>41</sup> The degree of alteration was determined by contact angle measurements.<sup>42,43</sup> Silane was used to coat glass slides to form a stable hydrophobic surface.<sup>44</sup> The glass slides were immersed in the oil bath and aged in a vacuum oven at 80 °C for 4 days. After that, the slides were washed with DI water and dried at 80 °C in the vacuum oven for 2 days. Wettability was determined by the sessile drop technique. A drop of the solution was placed on the glass slide and recording of the contact angle was started for a period of 55 min. For each data point, the average of 124 contact angle measurements taken

over 10 s is reported. In some measurements, the drop would wet the surface completely after 55 min at which point, it was no longer possible to capture the contact angle. The degree at which the drop spreads over the surface is utilized to indicate the efficiency of the delivery system in altering the wettability.

**IFT Measurements.** The IFT is a useful indication of how the capillary forces between oil and water change in the presence of an active material. The capillary number is defined as the ratio of viscous drag forces to IFT forces. Reducing the IFT by adding surfactants could aid in overcoming the capillary forces, thereby improving the oil recovery.<sup>1,7,39</sup>

An SDT by Kruss was used to measure the IFT. Measurements were made between 25 and 80 °C. The drop shape was fitted by the Young–Laplace model and the IFT was calculated by the ADVANCE software. The average of the last three measurements after stabilization of the IFT is reported. Dodecane is used as the light phase and HSW brine as the heavy phase.

## RESULTS AND DISCUSSION

**Optimization of the Size of the Nanocapsules.** Several trials were necessary to optimize the size and morphology of the nanocapsules. When the mixture of reagents at 100 rpm for 2 h and then aged for 48 h, the resultant capsules, D\_1, exhibited an irregular shape with a size larger than 200 nm as shown by the TEM images (Figure 1a). To investigate

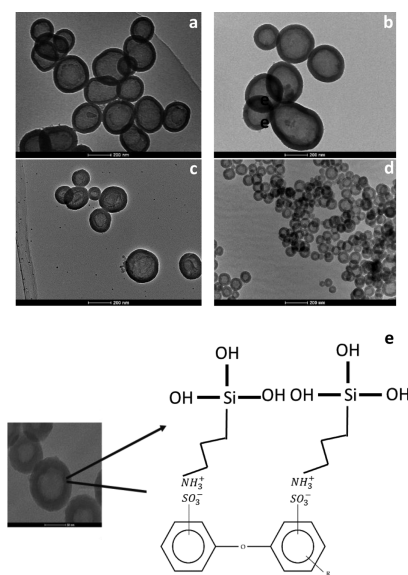


**Figure 1.** TEM images of the different nanocapsule systems. (a) D\_1, (b) D\_2, (c) D\_3, and (d) D\_4, (e) schematic of the interactions between the anionic surfactant and APTES, which is one of the silica precursors used in the synthesis.

the effects of the stirring on the shape and size of the particles, another synthesis was carried out with molar ratios similar to the above but maintaining a stirring speed of 100 rpm for 48 h. While the shape of the particle became mostly spherical (D\_2), the size remained larger than 200 nm, as shown in Figure 1b. For many practical applications, the size of the particles is important. For example, for subsurface applications where access to the smaller pores is necessary, it is desirable to use particles that are less than 100 nm. In addition to access issues, deployment of large-sized particles to a porous medium will result in plugging the pores with adverse effects in the oil recovery.<sup>45–48</sup> Further optimization by controlling the molar ratio of reactants led to smaller-sized particles. The D\_3 system results in spherical particles with a size of about 130 nm as shown in Figure 1c. Finally, D\_4 shows sub-100 nm particles with a uniform hollow spherical structure (Figure 1d). The size of the mesopores, as determined from the Brunauer–Emmett–Teller measurements and the BJH model, is 4.5 nm. Note that the mesopores are formed by templating around the anionic surfactant molecules. Thus, the surfactant is electrostatically bound inside the pores rather than physically adsorbed onto the surface. The ionic interactions between the positively charged aminopropyl group from APTES and the anionic head of the surfactant are shown schematically in Figure 1e.<sup>26,40</sup> Optimization of the amount of surfactant used in the synthesis as well as thorough washing of the product is necessary to minimize the presence of excess surfactant molecules that physically bind to the surface. It is also clear that the size of the particles depends greatly on the molar ratio of TEOS, APTES, and DOWFAX 2A1. In addition, the shape of the nanocapsules depends on the nucleation process, which is also a function of the TEOS/APTES/DOWFAX 2A1 ratio. The presence of ethanol in the mixture slows the hydrolysis rate of TEOS and APTES, which results in a kinetically controlled reaction. As seen from Table 2, as the amount of ETOH increases, the size of the particles decreases. Moreover, APTES can act as a catalyst that accelerates the hydrolysis process, which leads to larger-sized particles.<sup>40</sup> It could also be inferred from the table that when the amount of APTES was reduced, the size of the particles also became smaller. By controlling the particle size and further limiting the rate of nucleation by the stirring speed, we are able to produce sub-100 nm-sized capsules with DOWFAX 2A1 encapsulated into the hollow core. One interesting consequence of size control is the amount of DOWFAX 2A1 encapsulated. As shown in Figure S3, the amount of DOWFAX 2A1 encapsulated in D\_4 is 40 wt % compared to 30% in D\_1. Therefore, maintaining the stirring speed of 400 rpm for 24 h, carrying out the reaction at 70 °C for 2 h and then at 25 °C for 22 h with molar ratios of 1159/35.5/1/0.4/0.9 H<sub>2</sub>O/ETOH/DOWFAX 2A1/APTES/TEOS resulted in nanocapsules with a size less than 100 nm and a 40 wt % surfactant encapsulation.

**Slow Release of DOWFAX 2A1 Molecules.** As mentioned earlier, for successful implementation of cEOR, large quantities of the surfactant are needed to overcome adsorption, which leads to high cost. A potential solution is a system with slow and controlled release mechanism that ensures surfactant availability deeper in the subsurface formation. The surfactant release profiles of various systems in HSW brine are shown in Figure 2. For the large particles, the release reaches 14% even after a long period of time. In contrast, for the smaller size, the amount of release is higher. The D\_3 capsules show two distinct regimes. The first part,

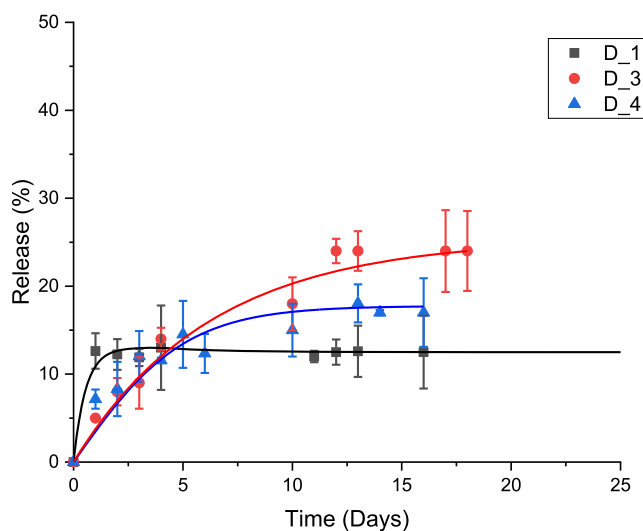


**Figure 2.** Release profile for DOWFAX 2A1 using different capsules at room temperature. The release of D\_1 reaches a quick plateau whereas D\_3 and D\_4 show a longer sustainable release.

within the first 5 days, is linear and releases 15% of the total amount of surfactant encapsulated. It is followed by a slower increase in surfactant concentration until it levels off at 25% after 20 days. D\_4 also follows a similar profile; it plateaus at 18% within the first 10 days and stays at that level for 18 days. Generally, the smaller the particles the better they disperse and hence they interact more with the ions in the solution. This could be one explanation for why the D\_3 and D\_4 profiles show a higher release in comparison to D\_1.

The rate of release was also studied at elevated temperatures closer to the conditions, which are normally encountered in the subsurface environment. Figure 3 shows clearly that the

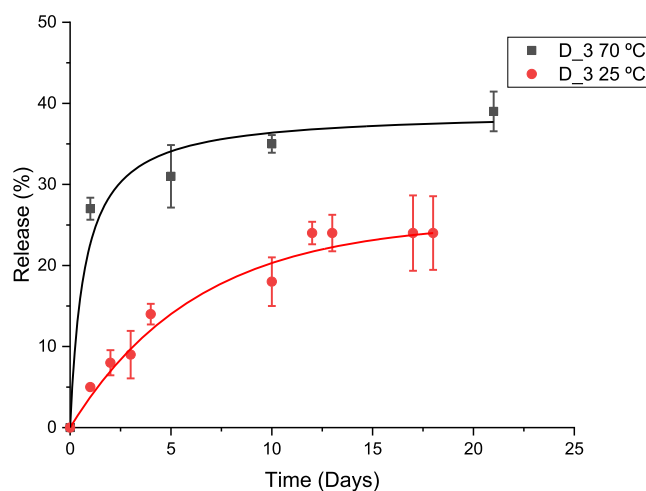


**Figure 3.** Comparison of the release profiles at room temperature and 70 °C.

release of the surfactant is enhanced at higher temperatures. The amount of the surfactant released is doubled compared to that released at room temperature. The enhanced release is likely to have resulted from the increase in diffusion as a result of the temperature increase.

The slow release profile is essential for subsurface applications. Nanoparticles require months to travel from an injector to a producer. In a recent field study,<sup>45,46</sup> fluorescent

nanoparticle tracers injected in a water injector required 50–200 days to be recovered from a producer that is 500 m away. For the nanosized capsules, only 40% of the surfactant is released within the first 20 days, followed by a much slower release rate, suggesting that they can reach deeper into the unswept reservoir areas and deliver surfactant molecules due to the slow-release kinetics.

**Wettability Alteration Performance.** The tendency of a fluid to adhere to a solid surface in the presence of another immiscible fluid defines its wettability. It is a crucial property when evaluating the multiphase flow in a rock matrix. It controls the distribution of oil and water in the reservoir and, hence, has a great impact on oil recovery.<sup>44</sup> If the contact angle of a water drop on a solid surface is above 90°, then the surface is considered oil-wet. Those with contact angles less than 90° are water-wet.<sup>5</sup> The change of the wettability from oil-wet to water-wet can significantly increase the capillary pressure, as shown by the well-known Young–Laplace equation.<sup>49</sup> The highest value of the capillary pressure results when the contact angle between the oil and water is zero.

The effectiveness of the system in altering the wettability is shown in Figure 5. When a drop of HSW is placed on the

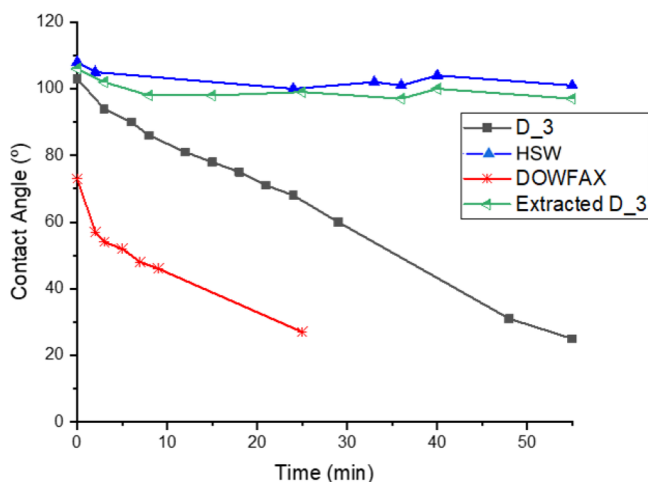


**Figure 4.** Contact angle vs time using the D\_3 nanocapsules and the neat surfactant. For comparison, the contact angle values of the nanocapsules from which the surfactant has been previously removed is also shown. The latter appears virtually identical to the HSW brine only, where no change is observed.

hydrophobic surface that is coated with oil, the contact angle remains constant at 103° over 55 min. However, when D\_3 was first suspended in HSW for 1 day and then a drop of the suspension was placed on the glass slide, the contact angle dropped linearly with time to below 30°, demonstrating that the released surfactant molecules are effective in altering the surface wettability. To prove that the mechanism for the wettability alteration is the slow release of the surfactant, the host capsules were tested after the surfactant molecules were removed from the system (D\_3) by calcination under N<sub>2</sub> at 600 °C for 6 h.<sup>40</sup> The results using the D\_3 capsules with the surfactant that have been first suspended for 1 day at room temperature, the surfactant-free capsules, and the neat surfactant (0.15 mg mL<sup>-1</sup>, which is the total concentration of the material encapsulated in 0.5 mg mL<sup>-1</sup> of D\_3) are shown in Figure 4. As can be seen, the surfactant-free capsules showed no major alteration of wettability, confirming that the

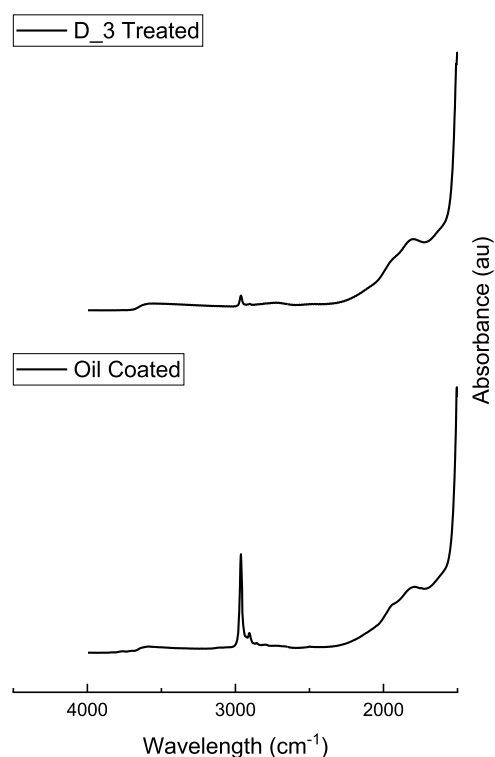


**Figure 5.** FT-IR spectra of a hydrophobic glass slide before (bottom) and after treatment with D\_3 nanocapsules in HSW (top). The intensity of the peak due to the alkyl groups from the oil is reduced significantly after treatment due to the released surfactant.

released surfactant is primarily responsible for the observed changes.

The change in surface wettability utilizing an anionic surfactant is believed to be caused by the hydrophobic interactions between the surfactant and the oil layer coating the glass slide. It is assumed that one reason for the reduction in wettability is the formation of a bilayer of the surfactant with the hydrophilic part pointing upward. The anionic end of a water-soluble surfactant would end up facing toward the flow, creating a zone of hydrophilicity. Due to the strong hydrophilic interactions, the surfactant will push and displace the oil that coats the glass surface. A similar mechanism was proposed by Nguyen et al. for nonionic surfactants.<sup>50</sup> However, in our system, there are two major interactions to consider. Since the silica nanocapsules are hydrophilic, they are not expected to interact strongly with a hydrophobic surface. Thus, other mechanisms based, for example, on the disjoining pressure have been proposed.<sup>51</sup> Nevertheless, the nanoparticles could still exert a force on the surface of the oil phase, creating a high-pressure and velocity potential zone that pushes the oil aside. Moreover, the presence of the surfactant in the solution after it is released from the silica host might improve the hydrophobic interactions between the particles and the oil, which further can enable a better sweep of oil.

To further investigate the effect on the surface of the glass slides after treatment with D\_3, we used FTIR spectroscopy. The glass slides were soaked in a solution of D\_3 in HSW for 2 h. After that, the glass was dried in a vacuum oven at 80 °C for 3 days. The FT-IR spectra are shown in Figure 5. The peak intensity of CH<sub>2</sub> and CH<sub>3</sub> groups at ~2960 cm<sup>-1</sup>, which arises from the modification of the glass with the oil, is significantly

reduced after exposure to D\_3 nanocapsules in agreement with the contact angle measurements.

**IFT Experiments.** Another important indication of the applicability of a system to mobilize trapped oil is the reduction of the IFT between oil and water. Lowering the IFT has been reported to result in achieving a higher oil recovery.<sup>41</sup> IFT measurements were carried out to show the performance of the DOWFAX 2A1 containing nanocapsules over time and at elevated temperatures. The cmc of DOWFAX 2A1 in HSW brine was determined to be  $0.126 \text{ mg mL}^{-1}$  (Figure 6). Note

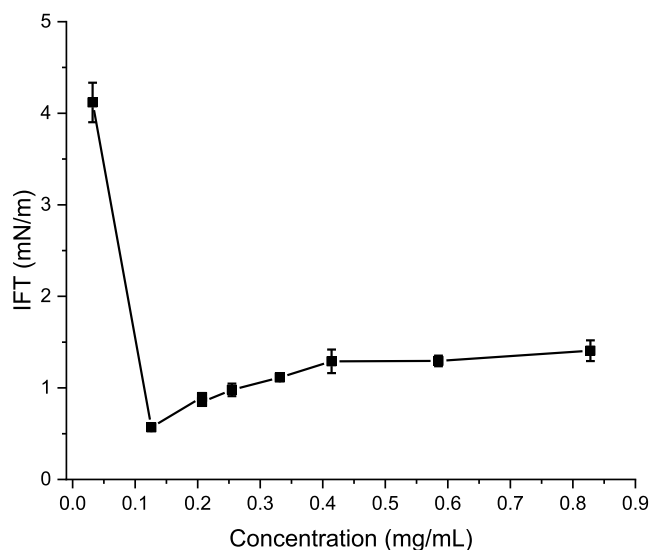


**Figure 6.** IFT vs concentration for DOWFAX 2A1 in HSW. The cmc calculated from the minimum in the plot is  $0.126 \text{ mg mL}^{-1}$ .

that the cmc value reported in 0.1 M NaCl is  $0.07 \text{ mg mL}^{-1}$ . The small difference is attributed to the different brine solutions used (0.1 M NaCl vs HSW) in the measurements. The figure shows a typical behavior for the IFT variation in the presence of the surfactant. Below the cmc, the surfactant molecules adsorb preferentially to the oil–water interface, which causes the IFT to reduce quickly to a minimum value of  $0.5 \text{ mN m}^{-1}$ . When the maximum adsorption is reached, further addition of surfactant molecules can form micelles, which does not contribute to further decreases of the IFT.<sup>52,53</sup> Note that the maximum concentration of surfactant available in the systems tested is  $0.15 \text{ mg mL}^{-1}$ , which suggests that the concentration of the surfactant in these experiments will be below the cmc.

Experimental studies have concluded that the oil saturation decreases when the capillary number increases.<sup>54</sup> The IFT of dodecane–HSW in the presence of D\_3 at 500 ppm in HSW for various hydrolysis times is shown in Figure 8. The surface tension of the HSW–dodecane system is  $62 \text{ mN m}^{-1}$ , as shown in Figure 7. After 3 days of immersion in HSW and surfactant release, the IFT of the dodecane–HSW mixture drops 10-fold, reducing from 62 to  $2.1 \text{ mN m}^{-1}$ . Moreover, as a result of the slow release of the surfactant, the IFT becomes lower as more surfactant is released from the nanocapsules. The system is expected to be functional for a long time when deployed for subsurface applications such as oil recovery, where it takes nanoparticles around a month to travel from an injector to a producer.<sup>45</sup> Recent work has shown that equilibrating surfactant molecules with crude oil results in an IFT increase due to the partitioning of the surfactant into the

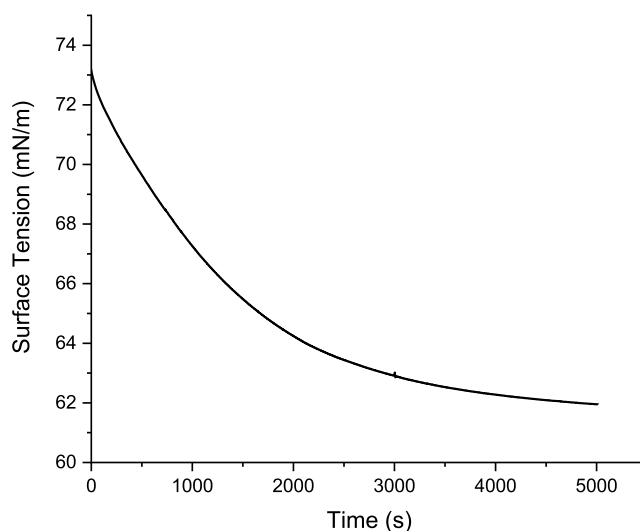


**Figure 7.** Surface tension of dodecane and HSW without the nanocapsules.

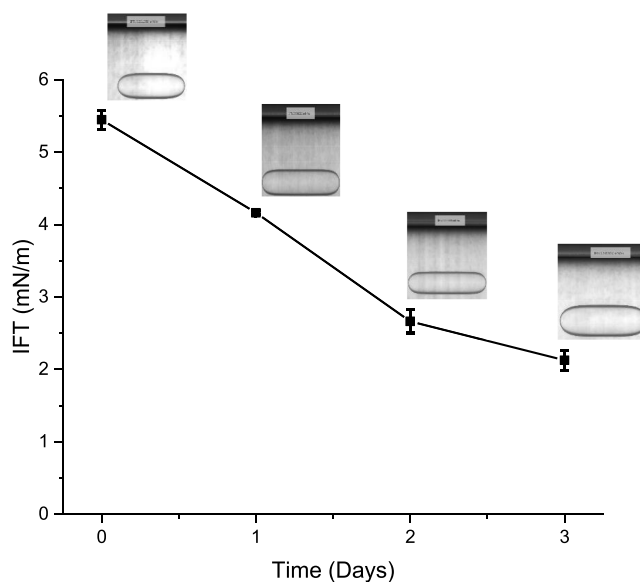


**Figure 8.** IFT measurements over time of dodecane HSW mixture after the addition of D\_3. The continuous decreases of IFT over time supports the sustainable release of the surfactant from the nanocapsules.

oil phase.<sup>55</sup> Hence, the slow release of the surfactant molecules could overcome this limitation by providing a fresh supply of surfactant molecules. Note that the release is only  $\sim 35\%$  of the total amount of surfactant encapsulated, which corresponds to  $0.05 \text{ mg mL}^{-1}$  surfactant released in the solution.

Subsurface environments, such as oil reservoirs, could have temperatures as high as  $100\text{--}120 \text{ }^\circ\text{C}$ .<sup>56</sup> Therefore, it is important to test the performance of the system also at elevated temperatures. Figure 9 shows clearly that the IFT is reduced at elevated temperatures. Similar to Figure 6, it shows a V-shaped plot as a result of having excess surfactant present in the solution. Diffusion of the surfactant is a thermally activated process and, therefore, it is enhanced at elevated temperatures as seen by the Stokes–Einstein equation

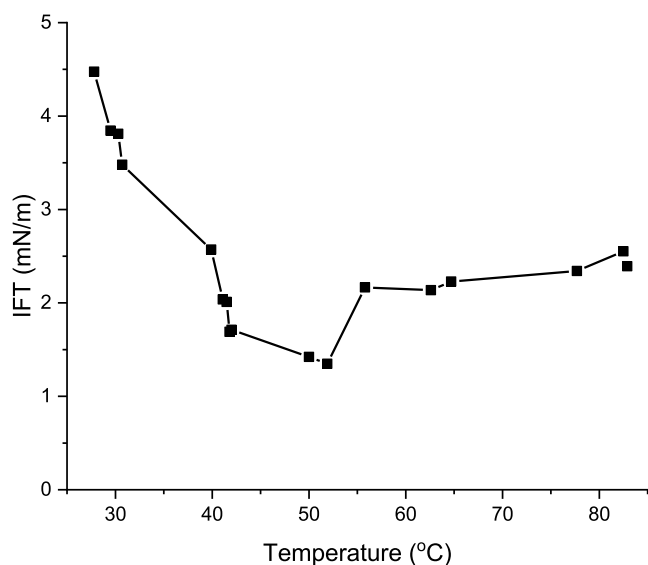


**Figure 9.** IFT as a function of temperature of dodecane–HSW after addition of D<sub>3</sub> nanocapsules.

$$D = \frac{K_b T}{6\pi\mu R} \quad (1)$$

where  $K_b$  is Boltzmann's constant ( $1.38 \times 10^{-23}$  J K<sup>-1</sup>),  $T$  is the temperature in degrees kelvin,  $R$  is the radius of the molecule or the particle if they are small enough to follow random motion.

## CONCLUSIONS

A new platform for slow release of an anionic surfactant (e.g., DOWFAX 2A1) has been demonstrated. The system is based on anionic surfactant molecules incorporated into sub-100 nm hollow sphere-like silica nanocapsules composed of a mesoporous shell. The size of the nanocapsules was optimized by varying the experimental parameters that affect typically the nucleation and growth during the synthesis reaction. The applicability of the system for hydrocarbon recovery applications and environmental remediation was demonstrated at both room and elevated temperatures in HSW. Moreover, the ability of the particles to alter the wettability of hydrophobic surfaces was tested and showed that the release of the surfactant is responsible for altering an oil-wet surface to a more favorable water-wet one. Finally, the IFT of a dodecane–HSW mixture was lowered by an order of magnitude by incorporating the nanocapsules in the HSW.

## ASSOCIATED CONTENT

### Supporting Information

The Supporting Information is available free of charge at <https://pubs.acs.org/doi/10.1021/acsomega.0c06094>.

Detailed calculation of release experiments, chemical formula of DOWFAX surfactants, UV–vis spectra of DOWFAX-2A1, and TGA of D<sub>1</sub>, D<sub>2</sub>, D<sub>3</sub>, and D<sub>4</sub> systems (PDF)

## AUTHOR INFORMATION

### Corresponding Author

Emmanuel P. Giannelis – Department of Materials Science and Engineering, College of Engineering, Cornell University,

Ithaca, New York 14853, United States; Email: [epg2@cornell.edu](mailto:epg2@cornell.edu)

## Authors

**Ahmed Wasel Alsmail** – Department of Chemical and Biomolecular Engineering, College of Engineering, Cornell University, Ithaca, New York 14853, United States; EXPEC Advanced Research Center, Saudi Aramco, Dhahran 31261, Saudi Arabia; [orcid.org/0000-0001-7121-9876](https://orcid.org/0000-0001-7121-9876)

**Mohammed Amen Hammami** – Department of Materials Science and Engineering, College of Engineering, Cornell University, Ithaca, New York 14853, United States

**Apostolos Enotiadis** – Department of Materials Science and Engineering, College of Engineering, Cornell University, Ithaca, New York 14853, United States

**Mazen Yousef Kanj** – College of Petroleum Engineering & Geosciences, King Fahd University of Petroleum and Minerals, Dhahran 31261, Saudi Arabia; [orcid.org/0000-0002-2674-4505](https://orcid.org/0000-0002-2674-4505)

Complete contact information is available at: <https://pubs.acs.org/10.1021/acsomega.0c06094>

## Author Contributions

A.W.A. conducted the experiments and wrote the draft for the manuscript. M.A.H. conducted the TEM imaging and reviewed and edited the manuscript. A.E. helped in suggesting the experiments to optimize the size of the nanocapsules. E.P.G. supervised the research, recommended experiments, and reviewed and edited the manuscript. M.Y.K. followed the research and reviewed and edited the manuscript.

## Notes

The authors declare no competing financial interest.

## ACKNOWLEDGMENTS

A.W.A. acknowledges the support of Saudi Aramco in sponsoring his studies at Cornell University. This publication is based on work supported by the College of Petroleum Engineering and Geosciences, King Fahd University of Petroleum and Minerals. We thank the Aramco Research Center—Boston—for the help with the IFT measurements. This work made use of the Cornell Center for Materials Research Shared Facilities, supported through the NSF MRSEC program (DMR-171987).

## REFERENCES

- Fletcher, P. D. I.; Savory, L. D.; Woods, F.; Clarke, A.; Howe, A. M. Model Study of Enhanced Oil Recovery by Flooding with Aqueous Surfactant Solution and Comparison with Theory. *Langmuir* **2015**, *31*, 3076–3085.
- Rosen, M. J.; Wang, H.; Shen, P.; Zhu, Y. Ultralow Interfacial Tension For Enhanced Oil Recovery At Very Low Surfactant Concentrations. *Langmuir* **2005**, *21*, 3749–3756.
- Kiani, S.; Rogers, S. E.; Sagisaka, M.; Alexander, S.; Barron, A. R. A New Class of Low Surface Energy Anionic Surfactant for Enhanced Oil Recovery. *Energy Fuels* **2019**, *33*, 3162–3175.
- Li, K.-x.; Jing, X.-q.; He, S.; Ren, H.; Wei, B. Laboratory Study Displacement Efficiency of Viscoelastic Surfactant Solution in Enhanced Oil Recovery. *Energy Fuels* **2016**, *30*, 4467–4474.
- Ayirala, S. C.; Boqmi, A.; Alghamdi, A.; AlSofi, A. Dilute Surfactants For Wettability Alteration And Enhanced Oil Recovery In Carbonates. *J. Mol. Liq.* **2019**, *285*, 707–715.
- Kamal, M. S.; Sultan, A. S.; Hussein, I. A. Screening Of Amphoteric And Anionic Surfactants For Ceor Applications Using A Novel Approach. *Colloids Surf, A* **2015**, *476*, 17–23.

- (7) Hirasaki, G. J.; Miller, C. A.; Puerto, M. Recent Advances in Surfactant EOR. *SPE Annual Technical Conference and Exhibition, Denver, Colorado, September 21–24, 2008*; Society of Petroleum Engineers, 2008.
- (8) ShamsiJazeyi, H.; Verduzco, R.; Hirasaki, G. J. Reducing Adsorption Of Anionic Surfactant For Enhanced Oil Recovery: Part II. Applied Aspects. *Colloids Surf., A* **2014**, *453*, 168–175.
- (9) Amirmoshiri, M.; Zhang, L.; Puerto, M. C.; Tewari, R. D.; Bahrim, R. Z. B. K.; Farajzadeh, R.; Hirasaki, G. J.; Biswal, S. L. Role of Wettability on the Adsorption of an Anionic Surfactant on Sandstone Cores. *Langmuir* **2020**, *36*, 10725–10738.
- (10) Li, K.; Jing, X.; He, S.; Wei, B. Static Adsorption and retention of Viscoelastic Surfactant in Porous Media: EOR Implication. *Energy Fuels* **2016**, *30*, 9089–9096.
- (11) Ma, K.; Cui, L.; Dong, Y.; Wang, T.; Da, C.; Hirasaki, G. J.; Biswal, S. L. Adsorption of cationic and anionic surfactants on natural and synthetic carbonate materials. *J. Colloid Interface Sci.* **2013**, *408*, 164–172.
- (12) Zhong, X.; Li, C.; Pu, H.; Zhou, Y.; Zhao, J. X. Increased Nonionic Surfactant Efficiency in Oil Recovery by Integrating with Hydrophilic Silica Nanoparticle. *Energy Fuels* **2019**, *33*, 8522–8529.
- (13) Wu, Y.; Chen, W.; Dai, C.; Huang, Y.; Li, H.; Zhao, M.; He, L.; Jiao, B. Reducing Surfactant Adsorption on Rock by Silica Nanoparticles for Enhanced Oil Recovery. *J. Pet. Sci. Eng.* **2017**, *153*, 283–287.
- (14) Kittirisawai, S.; Romero-Zerón, L. B. Complexation of Surfactant/ $\beta$ -Cyclodextrin to Inhibit Surfactant Adsorption onto Sand, Kaolin, and Shale for Applications in Enhanced Oil Recovery Processes. Part II: Dynamic Adsorption Analysis. *J. Surfactants Deterg.* **2015**, *18*, 783–795.
- (15) Fang, Z.; Cao, X.-R.; Yu, Y.-L.; Li, M. Fabrication and characterization of microcapsule encapsulating EOR surfactants by microfluidic technique. *Colloids Surf., A* **2019**, *570*, 282–292.
- (16) Rosestolato, J. C. S.; Pérez-Gramatges, A.; Lachter, E. R.; Nascimento, R. S. V. Lipid Nanostructures as Surfactant Carriers for Enhanced Oil Recovery. *Fuel* **2019**, *239*, 403–412.
- (17) Cortés, F.; Lozano, M.; Santamaria, O.; Betancur Marquez, S.; Zapata, K.; Ospina, N.; Franco, C. Development and Evaluation of Surfactant Nanocapsules for Chemical Enhanced Oil Recovery (EOR) Applications. *Molecules* **2018**, *23*, 1523.
- (18) Slowing, I. I.; Trewyn, B. G.; Giri, S.; Lin, V. S.-Y. Mesoporous Silica Nanoparticles For Drug Delivery And Biosensing Applications. *Adv. Funct. Mater.* **2007**, *17*, 1225–1236.
- (19) Tukappa, A.; Ultimo, A.; de la Torre, C.; Pardo, T.; Sancenón, F.; Martínez-Mañez, R. Polyglutamic Acid-Gated Mesoporous Silica Nanoparticles For Enzyme-Controlled Drug Delivery. *Langmuir* **2016**, *32*, 8507–8515.
- (20) Tang, F.; Li, L.; Chen, D. Mesoporous Silica Nanoparticles: Synthesis, Biocompatibility And Drug Delivery. *Adv. Mater.* **2012**, *24*, 1504–1534.
- (21) Chen, F.; Gong, A. S.; Zhu, M.; Chen, G.; Lacey, S. D.; Jiang, F.; Li, Y.; Wang, Y.; Dai, J.; Yao, Y.; et al. Mesoporous, Three-Dimensional Wood Membrane Decorated With Nanoparticles For Highly Efficient Water Treatment. *ACS Nano* **2017**, *11*, 4275–4282.
- (22) Hammami, M. A.; Croissant, J. G.; Francis, L.; Alsaiani, S. K.; Anjum, D. H.; Ghaffour, N.; Khashab, N. M. Engineering Hydrophobic Organosilica Nanoparticle-Doped Nanofibers For Enhanced And Fouling Resistant Membrane Distillation. *ACS Appl. Mater. Interfaces* **2017**, *9*, 1737–1745.
- (23) Lu, M.; Wang, A.; Li, X.; Duan, X.; Teng, Y.; Wang, Y.; Song, C.; Hu, Y. Hydrodenitrogenation of Quinoline Catalyzed by MCM-41-Supported Nickel Phosphides. *Energy Fuels* **2007**, *21*, 554–560.
- (24) Jana, S.; Dutta, B.; Bera, R.; Koner, S. Anchoring Of Copper Complex In MCM-41 Matrix: A Highly Efficient Catalyst For Epoxidation Of Olefins By tert-BuOOH. *Langmuir* **2007**, *23*, 2492–2496.
- (25) Alsaiani, S. K.; Hammami, M. A.; Croissant, J. G.; Omar, H. W.; Neelakanda, P.; Yapici, T.; Peinemann, K.-V.; Khashab, N. M. Colloidal Gold Nanoclusters Spiked Silica Fillers in Mixed Matrix Coatings: Simultaneous Detection and Inhibition of Healthcare-Associated Infections. *Adv. Healthcare Mater.* **2017**, *6*, 1601135.
- (26) Kim, S.-N.; Son, W.-J.; Choi, J.-S.; Ahn, W.-S. CO<sub>2</sub> adsorption using amine-functionalized mesoporous silica prepared via anionic surfactant-mediated synthesis. *Microporous Mesoporous Mater.* **2008**, *115*, 497–503.
- (27) de Freitas, F. A.; Keils, D.; Lachter, E. R.; Maia, C. E. B.; Pais da Silva, M. I.; Veiga Nascimento, R. S. Synthesis And Evaluation Of The Potential Of Nonionic Surfactants/Mesoporous Silica Systems As Nanocarriers For Surfactant Controlled Release In Enhanced Oil Recovery. *Fuel* **2019**, *241*, 1184–1194.
- (28) Alsmail, A. W.; Enotiadis, A.; Hammami, M. A.; Giannelis, E. P. Slow Release of Surfactant Using Silica Nanosized Capsules. *SPE J.* **2020**, *25*, 3472–3480.
- (29) Vallet-Regi, M.; Rámila, A.; del Real, R. P.; Pérez-Pariente, J. A. New Property Of MCM-41: Drug Delivery System. *Chem. Mater.* **2001**, *13*, 308–311.
- (30) Wang, A.; Kabe, T. Fine-Tuning Of Pore Size Of MCM-41 By Adjusting The Initial Ph Of The Synthesis Mixture. *Chem. Commun.* **1999**, 2067–2068.
- (31) Lin, X.-J.; Zhong, A.-Z.; Sun, Y.-B.; Zhang, X.; Song, W.-G.; Lu, R.-W.; Cao, A.-M.; Wan, L.-J. In Situ Encapsulation Of Pd Inside The MCM-41 Channel. *Chem. Commun.* **2015**, *51*, 7482–7485.
- (32) Wang, S.; Wang, K.; Dai, C.; Shi, H.; Li, J. Adsorption of Pb<sup>2+</sup> on amino-functionalized core-shell magnetic mesoporous SBA-15 silica composite. *Chem. Eng. J.* **2015**, *262*, 897–903.
- (33) Jahandar Lashaki, M.; Sayari, A. CO<sub>2</sub> Capture Using Triamine-Grafted SBA-15: The Impact Of The Support Pore Structure. *Chem. Eng. J.* **2018**, *334*, 1260–1269.
- (34) Kruk, M.; Jaroniec, M.; Ko, C. H.; Ryoo, R. Characterization Of The Porous Structure Of SBA-15. *Chem. Mater.* **2000**, *12*, 1961–1968.
- (35) Shiau, B.-J.; Rouse, J. D.; Sabatini, D. A.; Harwell, J. H. Surfactant selection for optimizing surfactant-enhanced subsurface remediation. *ACS Symp. Ser.* **1995**, *594*, 65–79.
- (36) Deshpande, S. DOWFAX Surfactant Components For Enhancing Contaminant Solubilization. *Water Res.* **2000**, *34*, 1030–1036.
- (37) Nivas, B. T.; Sabatini, D. A.; Shiau, B.-J.; Harwell, J. H. Surfactant Enhanced Remediation Of Subsurface Chromium Contamination. *Water Res.* **1996**, *30*, 511–520.
- (38) *Surfactants in Solution. Theoretical and Applied Aspects*; Mittal, K. L., Lindman, B., Eds.; Plenum Press: New York, 1984.
- (39) Abdel-Fattah, A. I.; Mashat, A.; Alaskar, M.; Gizzatov, A. NanoSurfactant for EOR in Carbonate Reservoirs. *SPE Kingdom of Saudi Arabia Annual Technical Symposium and Exhibition, Dammam, Saudi Arabia, April 24–27, 2017*; Society of Petroleum Engineers, 2017.
- (40) Han, L.; Gao, C.; Wu, X.; Chen, Q.; Shu, P.; Ding, Z.; Che, S. Anionic Surfactants Templating Route For Synthesizing Silica Hollow Spheres With Different Shell Porosity. *Solid State Sci.* **2011**, *13*, 721–728.
- (41) Wang, Y.; Xu, H.; Yu, W.; Bai, B.; Song, X.; Zhang, J. Surfactant Induced Reservoir Wettability Alteration: Recent Theoretical And Experimental Advances In Enhanced Oil Recovery. *Pet. Sci.* **2011**, *8*, 463–476.
- (42) Gbadamosi, A. O.; Junin, R.; Manan, M. A.; Agi, A.; Oseh, J. O.; Usman, J. Synergistic Application Of Aluminium Oxide Nanoparticles And Oilfield Polyacrylamide For Enhanced Oil Recovery. *J. Pet. Sci. Eng.* **2019**, *182*, 106345.
- (43) Kanj, M.; Sakthivel, S.; Giannelis, E. Wettability Alteration In Carbonate Reservoirs By Carbon Nanofluids. *Colloids Surf., A* **2020**, *598*, 124819.
- (44) Al-Anssari, S.; Barifcani, A.; Wang, S.; Maxim, L.; Iglauer, S. Wettability Alteration Of Oil-Wet Carbonate By Silica Nanofluid. *J. Colloid Interface Sci.* **2016**, *461*, 435–442.
- (45) Alaskar, M.; Kosynkin, D. Successful Crosswell Field Test Of Fluorescent Carbogenic Nanoparticles. *J. Pet. Sci. Eng.* **2017**, *159*, 443–450.

(46) Kanj, M.; Rashid, M.; Giannelis, E. Industry First Field Trial of Reservoir Nanoagents. *SPE Middle East Oil and Gas Show and Conference, September 25–28, Manama, Bahrain*; Society of Petroleum Engineers, 2011.

(47) Kanj, M. Y.; Kosynkin, D. V. Oil industry first field trial of interwell reservoir nanoagent tracers. *Micro- and Nanotechnology Sensors, Systems, and Applications VII*; International Society for Optics and Photonics, 2015; 94671D.

(48) Kanj, M. Y.; Funk, J. J.; Al-Yousif, Z. Nanofluid coreflood experiments in the ARAB-D. *SPE Saudi Arabia Section Technical Symposium, Alkhobar, Saudi Arabia, May 9–11, 2009*; Society of Petroleum Engineers, 2009.

(49) Grate, J. W.; Dehoff, K. J.; Warner, M. G.; Pittman, J. W.; Wietsma, T. W.; Zhang, C.; Oostrom, M. Correlation Of Oil–Water And Air–Water Contact Angles Of Diverse Silanized Surfaces And Relationship To Fluid Interfacial Tensions. *Langmuir* **2012**, *28*, 7182–7188.

(50) Das, S.; Nguyen, Q.; Patil, P. D.; Yu, W.; Bonnezaze, R. T. Wettability Alteration Of Calcite By Nonionic Surfactants. *Langmuir* **2018**, *34*, 10650–10658.

(51) Wasan, D.; Nikolov, A.; Kondiparty, K. The wetting and spreading of nanofluids on solids: Role of the structural disjoining pressure. *Curr. Opin. Colloid Interface Sci.* **2011**, *16*, 344–349.

(52) Yuan, C.-D.; Pu, W.-F.; Wang, X.-C.; Sun, L.; Zhang, Y.-C.; Cheng, S. Effects of Interfacial Tension, Emulsification, and Surfactant Concentration on Oil Recovery in Surfactant Flooding Process for High Temperature and High Salinity Reservoirs. *Energy Fuels* **2015**, *29*, 6165–6176.

(53) Belhaj, A. F.; Elraies, K. A.; Alnarabiji, M. S.; Shuhli, J. A. B. M.; Mahmood, S. M.; Ern, L. W. Experimental Investigation of Surfactant Partitioning in Pre-CMC and Post-CMC Regimes for Enhanced Oil Recovery Application. *Energies* **2019**, *12*, 2319.

(54) Sheng, J. J. Status Of Surfactant EOR Technology. *Petroleum* **2015**, *1*, 97–105.

(55) Chung, J.; Boudouris, B. W.; Franses, E. I. Effects of the water-oil volume ratio and premixing or pre-equilibration on the interfacial tension and phase behavior of biphasic mixtures. *Colloids Surf., A* **2019**, *571*, 55–63.

(56) Mashat, A.; Gizzatov, A.; Abdel-Fattah, A. Novel Nano-Surfactant formulation to overcome key drawbacks in conventional chemical EOR technologies. *SPE Asia Pacific Oil and Gas Conference and Exhibition, Brisbane, Australia. October 23–25, 2018*; Society of Petroleum Engineers, 2018.